Hetero-Diels–Alder Ligation (HDAL) of C_{20} Nanocage and Anti-Tumor Oxoindoline in Gas Phase and Solvent Phase, Using Density Functional Theory (DFT)

Poor Heravi, Mohammad Reza; Habibzadeh, Sepideh
Department of Chemistry, Payame Noor University, Tehran, I.R. IRAN

Shoaei, Seyed Mohammad*[+]
Department of Chemistry, Zanjan Branch, Islamic Azad University, Zanjan, I.R. IRAN

Rahmani, Zahra*[+]
Department of Chemistry, Tabriz Branch, Islamic Azad University, Tabriz, I.R. IRAN

Ebadi, Abdol Ghaffar
Department of Agriculture, Jouybar Branch, Islamic Azad University, Jouybar, I.R. IRAN

Mert, Nihat; Mert, Handan
Department of Biochemistry, University of Yuzuncu Yil, 65080, Van, TURKEY

ABSTRACT: *In this computational research, the solvent effect is probed on HDAL of C_{20} with I to yield I_a compound. So, in going from the gas phase to non-polar, and in turn to the polar solvent, a good consistency appears between the dielectric constant of the solvent (ε) and the released solvation energy ($\Delta E_{l\text{-}g}$). The stability and polarity of I_a appearances are proportional to ε, and the probability of the H-bonding. While the obtained endo-isomer from HDAL is anticipated thermodynamically more stable than exo- analogue; here we found that the formation of exo-isomer is only the obtained product from this HDAL. Subsequently, exo-isomer is more stable than endo-analogue; due to the disappearance of the resulting electronic effect and ring-strain effect from π-stacking between the aromatic rings of I and nanocage. The possibility of HDAL is ruled out by the lowest energy barrier of 5.1 kcal/mol probed for exo Transition State (TS) in the gas phase, while the highest energy barrier of 9.4 kcal/mol is investigated for endo TS in H_2O. Hence, the designed HDAL is distinguished as an attractive and promising procedure for ligation in biochemistry due to its higher rate and selectivity in H_2O. Fascinatingly, similar to stable C_{60} nanostructure, exo HDAL of unstable C_{20} nanostructure with the scrutinized diene can be carried out thermally at room temperature and maybe a potential candidate for efficient and selective HDAL in living systems.*

KEYWORDS: *Dienophile; Diene; HDAL; Solvent effect; TS.*

***** *To whom correspondence should be addressed.*
+ E-mail: z.1401rahmani@gmail.com ; s_mohammadshoaei@yahoo.com
1021-9986/2023/2/369-380 12/$/6.02

INTRODUCTION

The HDAL is a way for yielding six-membered cyclic organic compound with boat conformation [1]. The biologically active compounds of C_{60} have been subject of intense research, for their chemistry and technological applications in different sciences. They are significantly coupled with geometry, stability and electronic properties in aqueous media [2,3]. Also, oxindole, and thioindoles are significant in biological testing and activity against for bacteria, viruses, cancer, malaria, and another diseases targeting exclusive enzymes [4-8]. *Gassman et al.* developed a simple one pot reaction for synthesis of indoles, isatins and their derivatives (Scheme 1) [5].

It was suggested that enamines and iminium salts are generally intermediates in the amine-catalyzed reactions of oxindoles with carbonyl compounds; and "Et_3N" is used in this reaction as a suitable base. Several experimental and theoretical attempts have been made on possible reactions between nanostructures with various species undergoing HDAL, functionalization, and so forth [9-15]. Nevertheless, there is no report on HDAL between **C_{20}** and **I** (Fig. 1).

Here, the characterization of HDAL are surveyed in the various solvents, using DFT—SCRF. We have chosen a B3LYP method in order to account for electron correlation effects and the large basis sets of wave functions (6-311++G** and AUG-cc-pVTZ) which support both polar and diffuse functions on hydrogen and heavy atoms. This seems to be a reasonable choice for the studied polar molecule which includes N, O, S atoms bearing lone pair electrons and H—bonding.

COMPUTATIONAL METHODS

Full optimizations of the scrutinized geometries are accomplished by GAMESS program, at the above-mentioned method and levels [16-19]. The TSs are found through the QST3 (reactants-products quasi-synchronous transit) manner [20]. The frequency computation is applied to characterize structure nature as minimum and/or maximum energy [21]. The solvent effect is studied by means of SCRF [22]. The AIM (atoms in molecules), NBO (natural bond orbital) and MEP (molecular electrostatic potential) calculations are carried out, too [23].

RESULTS AND DISCUSSION

Here, force constant calculations are carried out, where initial structures (**I** & **C_{20}**) as well as **I_a** are found as real minimum. Solvents with larger ε including H_2O, DMSO, and CH_3NO_2 that fall into the polar class are very effective at stabilizing minima and TSs (Figs. 2-3).

By changing media from gas phase to solvent phase, $E_{exo}^{\neq}$ and $E_{endo}^{\neq}$ is increased slightly. Even though the stabilizing effect of benzene is less than polar solvents and the $E_{exo}^{\neq}$ is decreased to 8.2, 7.1, 6.8, 6.3, 6.0, 5.4, and 5.1 kcal/mol, whereas the $E_{endo}^{\neq}$ is still too high (9.4, 8.8, 8.5, 8.0, 7.3, 6.9 and 5.5 kcal/mol, for H_2O, DMSO, CH_3NO_2, $C_2H_4Cl_2$, EtOH, C_6H_6, and gas phase, respectively). Evidently, the highest energy is related to *endo* TS in water, whereas the lowest energy is associated with *exo* TS in the gas phase (9.4 *vs.* 5.1 kcal/mol, correspondingly). The stability of solutes depends on solvent's ε and the possibility of H—bonding. Accordingly, the formation of the *endo* TS is expected to be energetically less favorable due to the π-π stacking between diene and dienophile. Generally, the cyclohexene ring in this process adopts an extended boat conformation. Since a folded boat conformation of this ring is predicted to be more stable in *exo* TS and less stable in *endo* TS, π-π aromatic stacking between the **C_{20}** and the diene are responsible for the TSs (Fig. S1). The stability ($\Delta E_{l\text{-}g}$) is useful to evaluate the solvent effects for chemical reactions and is consistent with the order of ε: $\Delta E_{b\text{-}g}$ [14.78] < $\Delta E_{d\text{-}g}$ [21.05] < $\Delta E_{e\text{-}g}$ [27.33] < $\Delta E_{n\text{-}g}$ [30.46] < $\Delta E_{d'\text{-}g}$ [34.92] < $\Delta E_{w\text{-}g}$ [36.74 kcal/mol]; also the reported ε is: $\varepsilon_{gas\ phase}$ [1] < $\varepsilon_{benzene}$ [2.2] < $\varepsilon_{dichloroethane}$ [10.4] < $\varepsilon_{ethanol}$ [24.6] < $\varepsilon_{nitromethane}$ [38.2] < ε_{DMSO} [46.7] < ε_{water} [78.4] (Fig. 4).

Moreover, the highest $|\Delta E_{l\text{-}g}|$ is observed in water (-36.74 kcal/mol), whereas the lowest $|\Delta E_{l\text{-}g}|$ is estimated in C_6H_6 (-14.78 kcal/mol). These results reveal more sensitivity of the stereoselective HDAL to stabilizing effects of more polar solvents *via* dipole-dipole interaction and H—bonding than less polar solvents or gas phase. The reasons are rather obvious. Firstly, there is a substituted pyrrole ring in **I** diene vertically which generates a relatively huge steric hindrance against *endo* direction of **C_{20}** dienophile, while this is not in the case *exo* direction of **I** and **C_{20}**. Secondly, there is a strong full conjugation (ring current) for non-bonding electrons of nitrogen with the neighboring carbonyl group of **I** diene. Because the *endo* isomer possesses a much higher energy than the *exo* isomer, henceforth structural parameter of the TSs imposes the stability of TSs and adduct. Interestingly, the dihedral angle of H—N and carbonyl group in TSs is about zero degree while this angle in adduct is estimated about

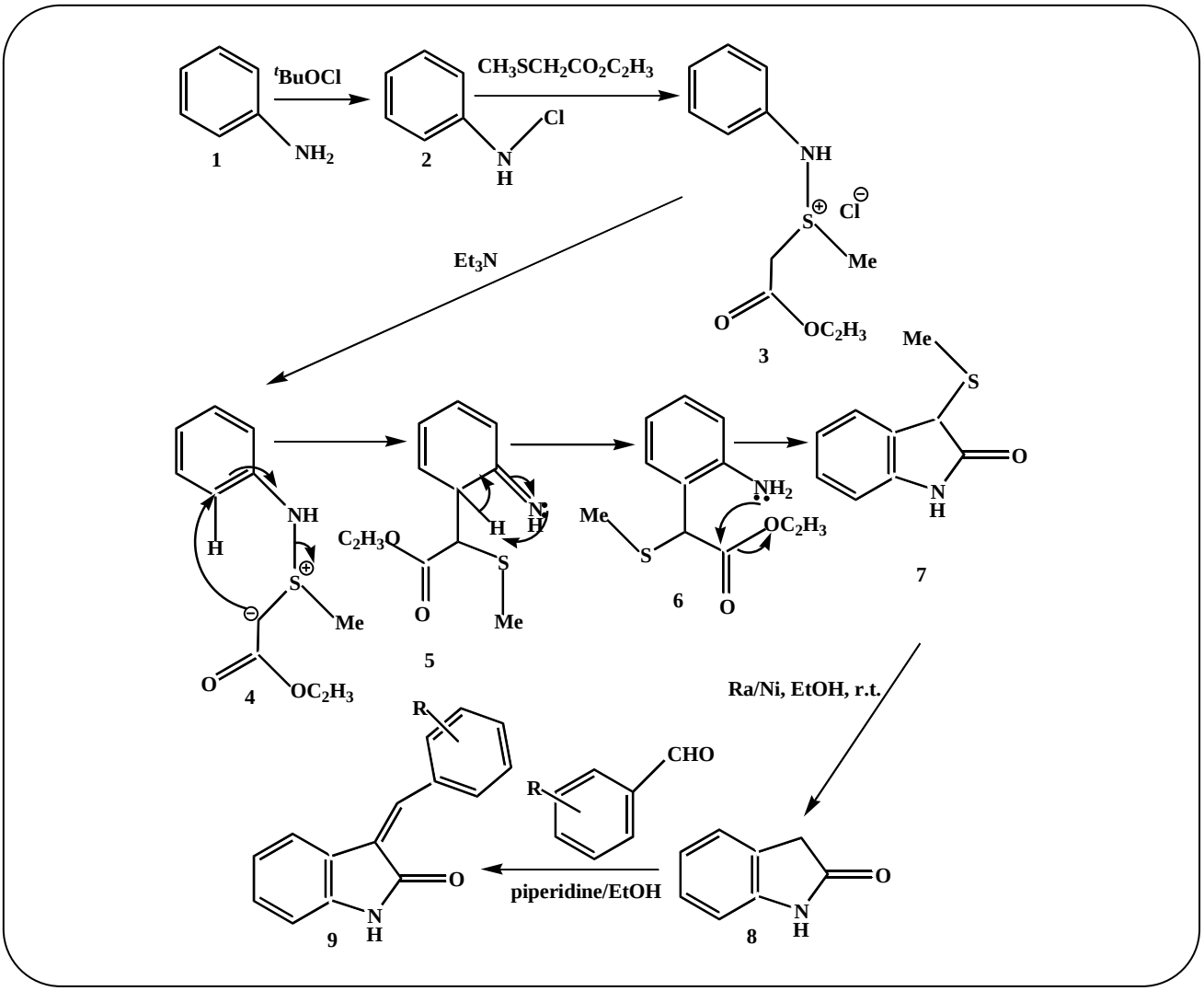

Scheme 1: The reported synthesis of 9.

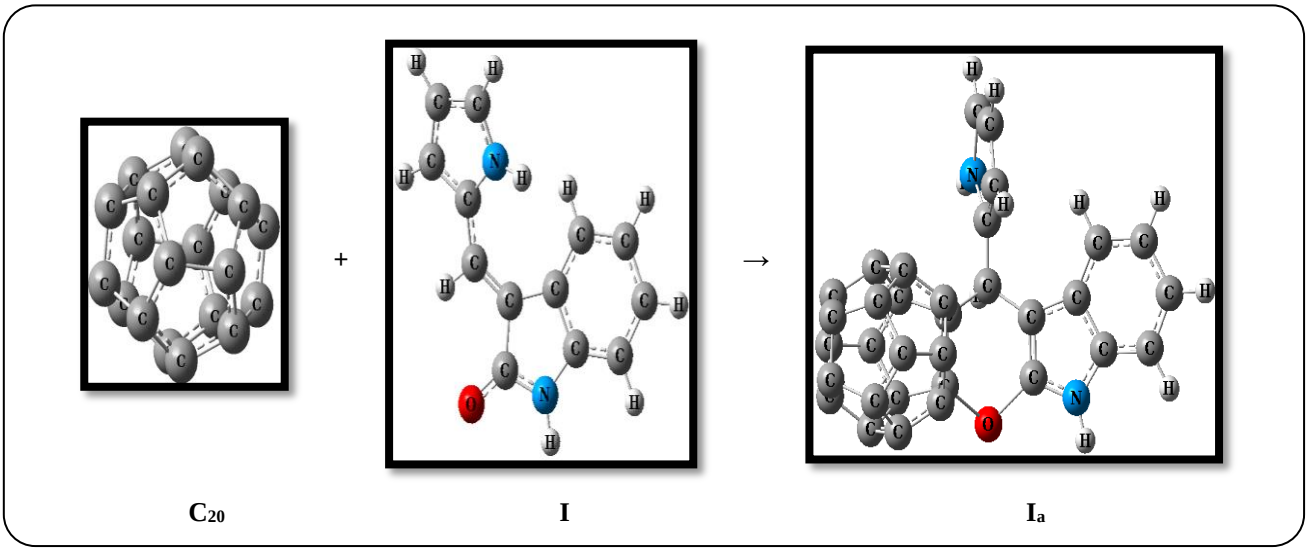

Fig. 1: The optimized C_{20}, I and I_a, using DFT—SCRF (self-consistent reaction field).

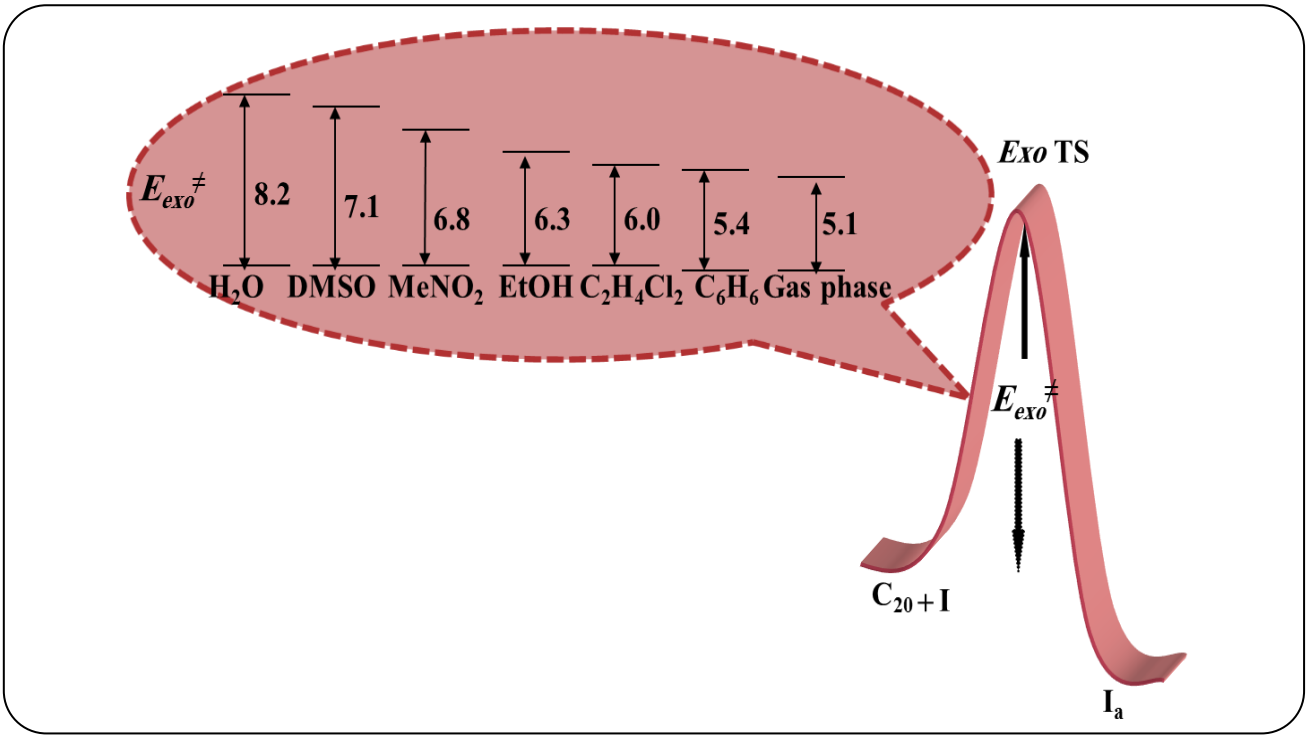

Fig. 2: The energy barrier of exo TS ($E_{exo}^{\neq}$) in seven media.

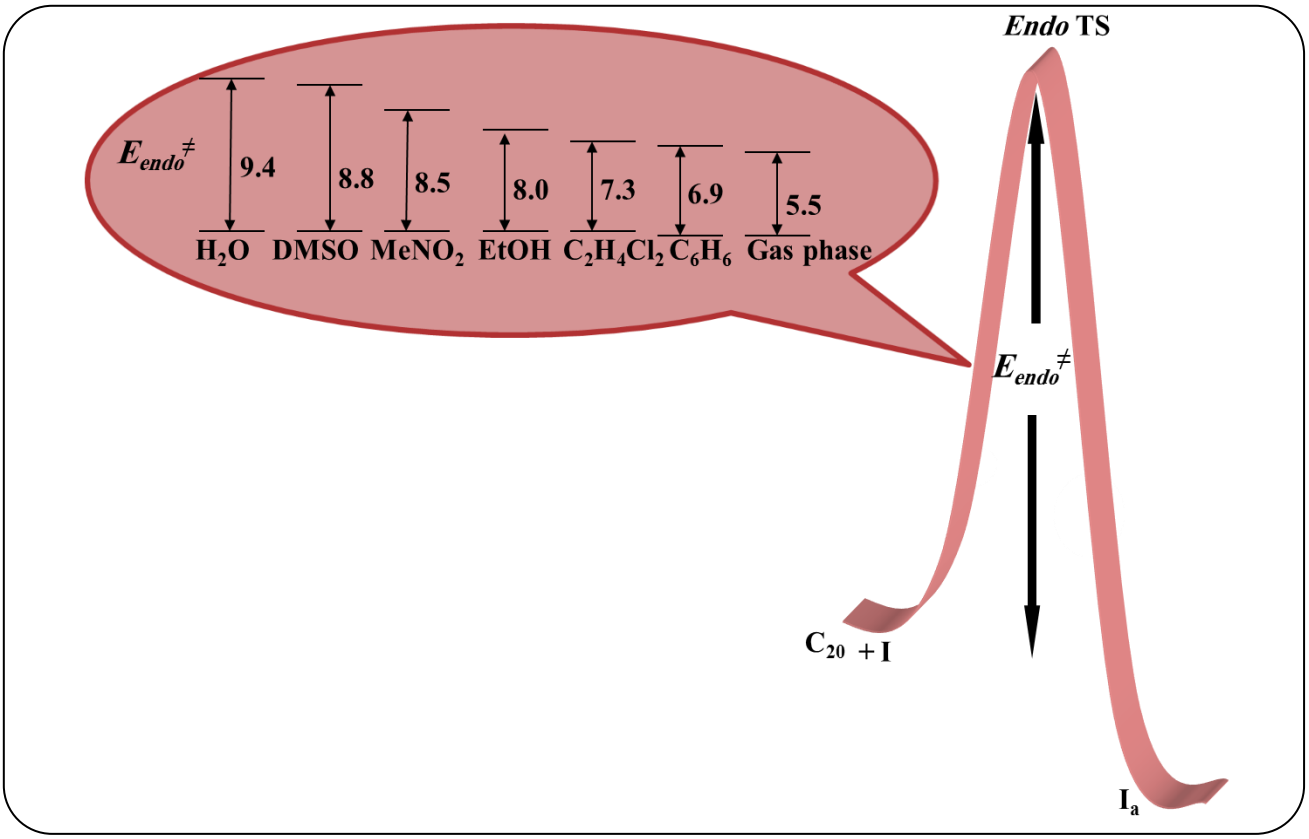

Fig. 3: The energy barrier of endo TS ($E_{endo}^{\neq}$) in seven media.

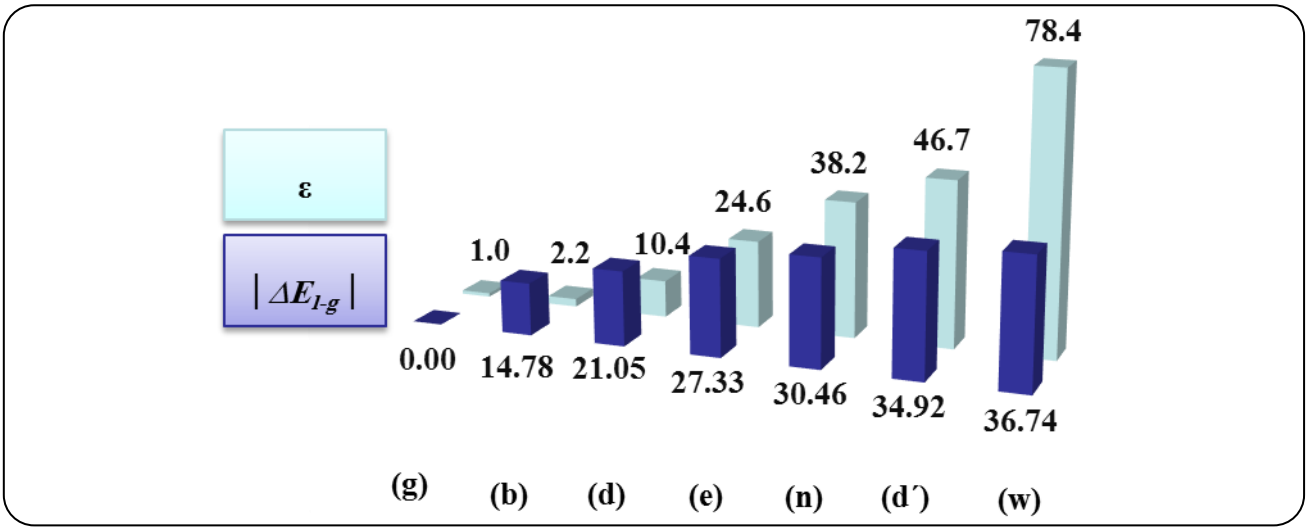

Fig. 4: Comparison of thermodynamic stability of I_a in seven media.

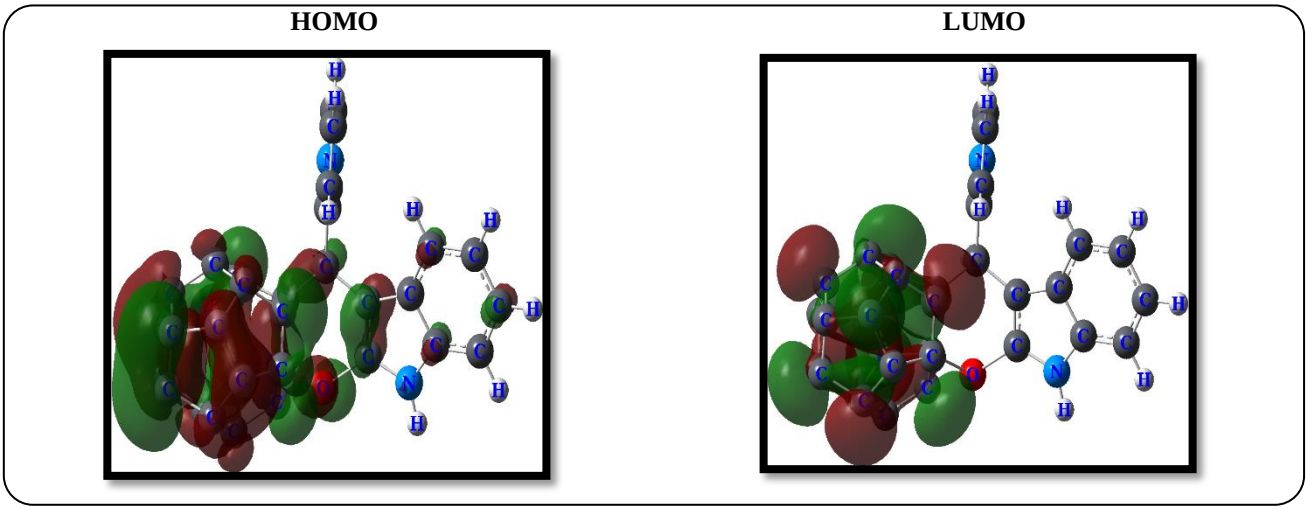

Fig. 5: The FMO (frontier molecular orbital) shapes of I_a, including HOMO-LUMO interaction (the highest occupied and the lowest unoccupied molecular orbital, respectively).

ten degree. This may be related to conjugation among the C=O and indoline. As said previously, the π-stacking is a further obstacle for *endo* attack. The last key question is what diastereomer is produced? Among the expected adducts of *exo* and *endo*; as two diastereomers, the formation of only one of two diastereomers is recommended through our theoretical scrutiny. As, the *endo* TS appears thermodynamically less reactive and more stable than its *exo* TS, the formation of the kinetically less reactive and more stable *exo* TS is suggested by reason of lack of π-stacking. The electron density ($\Sigma\rho_\pi$) at Bond Critical Points (BCPs) of $\mathbf{I_a}$ shows a linear correlation against the binding energy of $\Delta E = 724.58\ \Sigma\rho_\pi + 0.072$, displaying a reasonable correlation coefficient of r^2 (0.950), a standard deviation of SD (2.0 kJ/mol) and a strong bound complex of $\Sigma\rho_\pi$ (0.107). The estimated ΔE for *endo* TS is 77.60 kJ/mol, which is attributed to intermolecular BCPs. In various media, the structural parameter of $\mathbf{I_a}$ including point group, bond length, and bond angle is kept, while the dihedral angle is relatively modified (Table S1).

The changed dihedral angles between the substituted pyrrole ring and cyclohexene ring; D(10,26,38,39), D(10,26,38,40), D(23,26,38,39), D(23,26,38,40), D(10,26,38,45), and D(23,26,38,45); indicate, $\mathbf{I_a}$ structure is more sensitive to solvent effect through H—bonding and dipole-dipole interaction. The stereoselectivity of HDAL can be adjusted by molecular orbital theory (Fig. 5 and Scheme 2) [24-26].

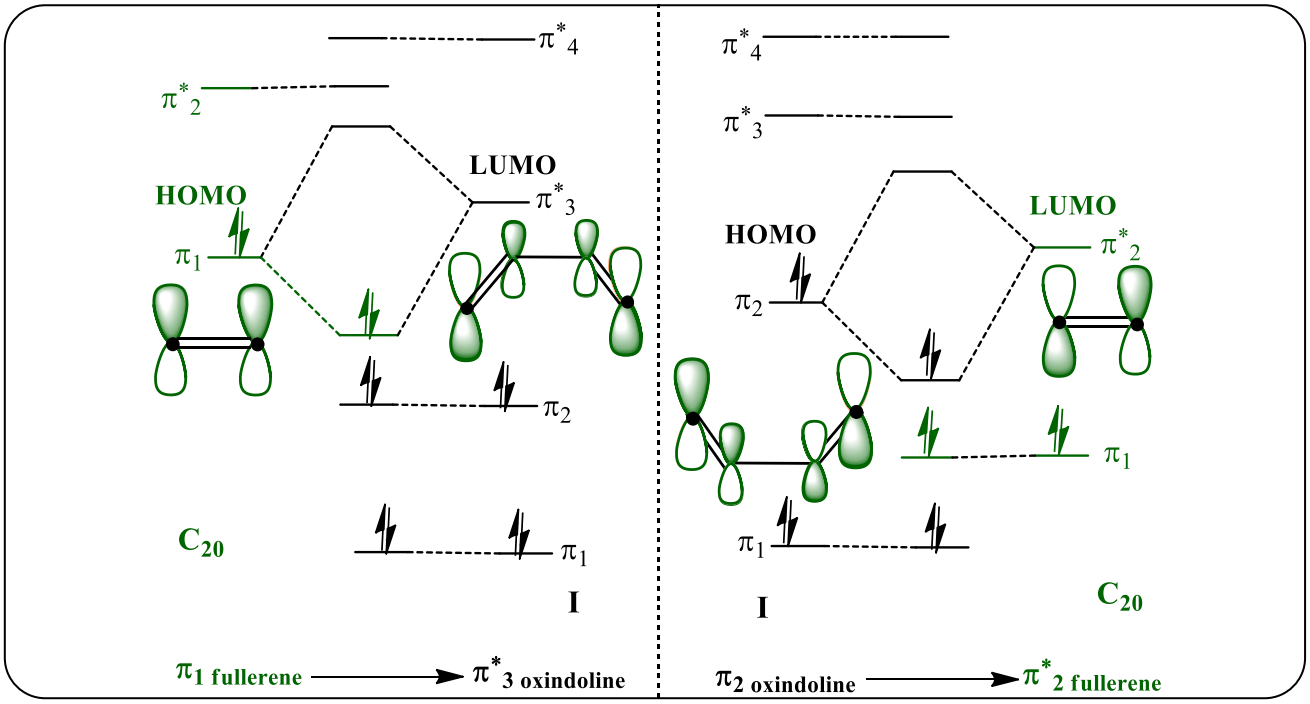

Scheme 2: The proposed FMO interactions of C20 with I.

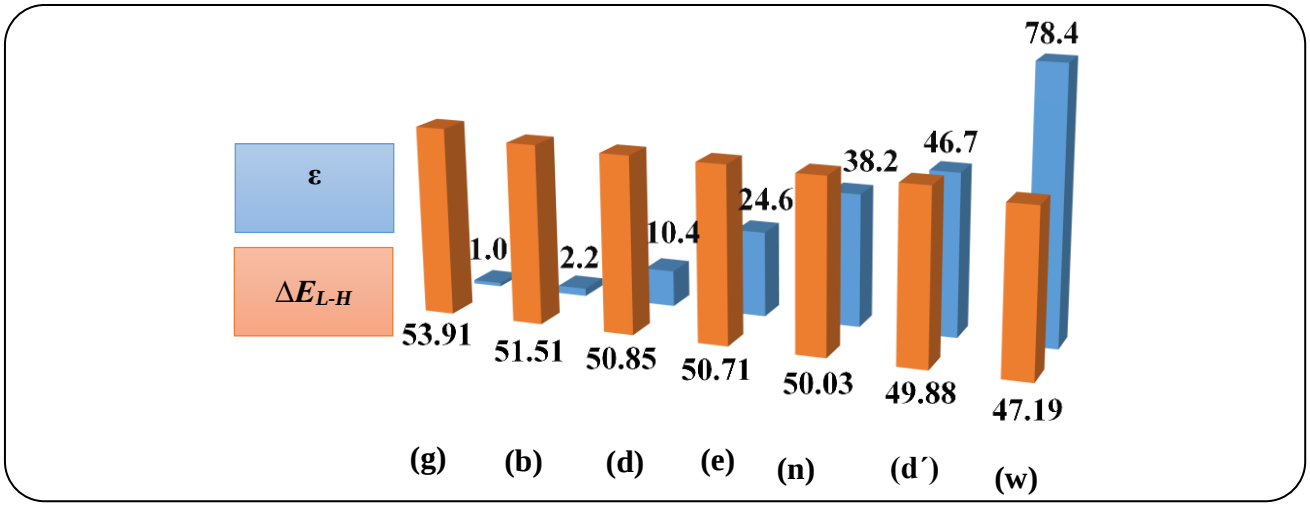

Fig. 6: Comparison of kinetic stability of Ia in seven media.

The FMO interaction of **C20** dienophile with **I** diene is proposed through the dienophile's π_1^2-orbital (or HOMO) → the diene's π^*_3-orbital (or LUMO), and/or the diene's π_2^2-orbital (or HOMO) → the dienophile's π^*_2-orbital (or LUMO).

The band gap ($\Delta E_{L\text{-}H}$ in kcal/mol) is calculated to reveal the solvent effect on kinetic stabilization of **Ia** and it is inconsistent with the order of ε: $\Delta E_{L\text{-}H}$ in the gas phase [53.91] < $\Delta E_{L\text{-}H}$ in C_6H_6 [51.51] < $\Delta E_{L\text{-}H}$ in $C_2H_4Cl_2$ [50.85] < $\Delta E_{L\text{-}H}$ in EtOH [50.71] < $\Delta E_{L\text{-}H}$ in $MeNO_2$ [50.03] < $\Delta E_{L\text{-}H}$ in DMSO [49.88] < $\Delta E_{L\text{-}H}$ in H_2O [47.19] (Fig. 6). In going from the gas phase to less polar solvent, then in turn to more polar solvent; the HOMO energy changes to a greater extent than the LUMO energy, thus there is an opposite direction between the order of $\Delta E_{L\text{-}H}$ and order of ε.

In other words, **Ia** is expected to be kinetically stabilized in the gas phase more than water. We have found that the solvent effect and stabilizing effect from gas phase to water causes the HOMO energy to decrease by 0.004 *a.u.;* the favorability of this HDAL increases as LUMO energy

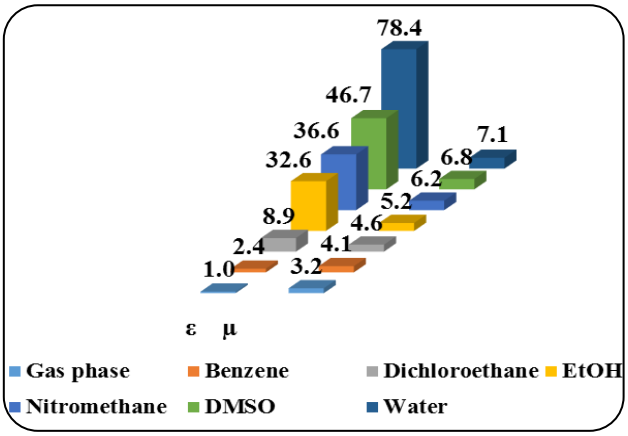

Fig. 7: Comparison of polarity of I_a in seven media.

decreases, meaning the band gap will be smaller, and electron transfer will be easily facilitated. The dipole moment (μ) of **I_a** structure is altered regularly with the enlarging polarity of the solvent (Fig. 7).

Again, the trend of μ / Debye for **I_a** is increased as: μ in the gas phase [3.81] < μ in benzene [4.82] < μ in dichloroethane [5.29] < μ in ethanol [5.35] < μ in nitromethane [6.08] < μ in DMSO [6.38] < μ in water [7.85], which is consistent with the order of ε. Henceforth, **I_a** because it's the highest μ in water, has the greatest affinity and interaction to this solvent. **I** reactant as one of Kekule''s compounds benefits from fully bonding resonance and shows a relatively high $\Delta E_{L\text{-}H}$ in the gas phase, while more polar solvent has a relatively low $\Delta E_{L\text{-}H}$, which leads to extremely high chemical reactivity. Additionally, shape, size, and values of the MEP of *exo* TS, *endo* TS, and **I_a** are charged for the positive sites *vs.* the negative sites, signifying blue color for H atoms and red color for other atoms, correspondingly (Fig. S2).

CONCLUSIONS

The results of DFT—SCRF calculations on the optimized (*E*)-3-1H-pyrrole-2-ylindoline-2-one[20] fullerene (**I_a**) in seven media, show:

(1) In going from the gas phase to non-polar, then in turn to the polar media, a rather good numerical consistency occurs between the ε and $\Delta E_{l\text{-}g}$. Moreover, the highest $\Delta E_{l\text{-}g}$ is observed in water (36.74 kcal/mol), whereas the lowest value is associated with benzene (14.78 kcal/mol). (2) Because of the capability of H—H-bonding, the stabilizing effect of water is greater than other solvents. (3) The band gap and kinetic stability emerge inconsistent with ε. (4) The π–π stacking leads to the destabilization of *endo* TS. (5) The dipolar interaction between **I** and polar solvent, leads to stability of *exo* TS and **I_a**. (6) The order of activation energy in seven media is followed: H_2O > DMSO > CH_3NO_2 > C_2H_5OH > $C_2H_4Cl_2$ > C_6H_6 > gas phase. (7) The calculated activation energy is low and the reaction is proposed to be synthetically interesting in the drug delivery field. (8) The highest activation energy for *endo* TS is 9.4 kcal/mol in water *vs.* 5.1 kcal/mol in the gas phase. (9) This is necessary for suggesting that only the most kinetically stable *exo* TS for HDAL is in the gas phase. (10) Regarding the MEP maps, the surveyed **I** and **C_{20}** are appropriately positioned to permit charge transfer between themselves. Therefore, the formation of two σ bonds takes place so rapidly without zwitterionic or di-radical intermediate; this HDAL is concerted and stereoselective, predicting only **I_a** product *via* stabilization of *exo* TS.

Supporting Information Available

The geometrical parameters of **I_a**, the optimized TSs, and their MEPs are presented (5 pages).

Received : Oct 30, 2022 ; Accepted : Jan. 16, 2023

REFERENCES

[1] (a) Azamat J., Poor Heravi M.R., Habibzadeh S., Ebadi A.G., Shoaei S.M., Vessally E., Hetero Diels–Alder Cycloadduct of Anti-Tumor (*E*)-3-X-indoline-2-thiones with C_{20} Fullerene as Drug Delivery in Solution *vs.* Gas Phase: A DFT survey, *Inorg. Chem. Commun.*, **139**:109353–109373 (2022).

(b) Matloubi Moghaddam F., Ghanbari B., Behzadi M., Baghersad M.H., Synthesis of Tetrahydrothiopyrano[2,3–b]indole [60]Fullerene Derivatives via Hetero-Diels–Alder Reaction of C_{60} and α,β-Unsaturated Indole-2–thiones, *J. Heterocycl. Chem.*, **54**:911–915 (2017).

(c) Klein D., "Organic Chemistry", Wiley, Hoboken NJ. 783 (2012).

[2] (a) Asnaashariisfahani M., Abdulkareem Mahmood E., Poor Heravi M.R., Habibzadeh S., Ebadi A.G., Mohammadi-Aghdam S., Solvent Effect on Cycloaddition of C20 nanofullerene with Indoline-2-One, at DFT, *J. Phys. Org. Chem.*, **35**: e4354–4374 (2022).

(b) Deguchi S., Alargova R.G., Tsujii K., Stable Dispersions of Fullerenes, C_{60} and C_{70}, in Water Preparation and Characterization, *Langmuir* **17**: 6013–6017 (2001).

[3] (a) Asnaashariisfahani M., Azizi B., Poor Heravi M.R., Habibzadeh S., Ebadi A.G., Ahmadi S., Stereoselective Cycloaddition of Biologically Active Thioindoline with the Smallest Nanocage in Gas Phase Vs. Solution via DFT, *J. Phys. Org. Chem.* **35**:e4390–4410 (2022).
(b) Liu Y., Wang H., Liang P., Zhang H.Y., Water-Soluble Supramolecular Fullerene Assembly Mediated by Metallobridged β-cyclodextrins, *Angew. Chem. Int. Ed.*, **43**:2690–4 (2004).

[4] (a) Kadhim M.M., Poor Heravi M.R., Mohammadi-Aghdam S., Habibzadeh S., Azizi B., Ebadi A.G., Shoaei S.M., Investigation of Anti-Tumor (*E*)-3-X-Oxindole *via* Functionalization of C_{20} Nano Structure: A DFT Approach, *Comput. Theor. Chem.* **1214**: 113763–113783 (2022).
(b) Vriens B.E.P.J., Aarts M.J.B., de Vries B., van Gastel S.M., Wals J., Smilde T.J., van Warmerdam L.J.C., de Boer M., van Spronsen D.J., Borm G.F., Tjan-Heijnen V.C.G., Breast Cancer Trialists' Group of the Netherlands (BOOG), Dox-Orubicin/Cyclophosphamide with Concurrent Versus Sequential Docetaxel as Neoadjuvant Treatment in Patients with Breast Cancer, *Eur. J. Cancer*, **49**: 3102–10 (2013).
(c) Sanna G., Pestrin M., Zafarana E., Biagioni C., Cavaciocchi D., Turner N., Di Leo A., Biganzoli L., Feasibility and Safety Of Dose-Dense Docetaxel after Conventional Epirubicin and Cyclophosphamide as Adjuvant Treatment for Early Breast Cancer Patients, *Breast*, **22**: 926–932 (2013).
(d) Thoenes L., Hoehn M., Kashirin R., Ogris M., Arnold G.J., Wagner E., Guenther M., In Vivo Chemo Resistance of Prostate Cancer in Metronomic Cyclophosphamide Therapy, *J. Proteomics* **73**:1342–54 (2010).

[5] (a) Gassman P.G., van Bergen T.J., Gruetzmacher G., Use of Halogen-Sulfide Complexes in the Synthesis of Indoles, Oxindoles, and Alkylated Aromatic Amines, *J. Am. Chem. Soc.* **95(19)**: 6508–6509 (1973).
(b) Gassman P.G., van Bergen T.J., Gilbert P.D., Jr Berkeley W.C., General Method for the Synthesis of Indoles, *J. Am. Chem. Soc.*, **96**: 5495–5508 (1974).
(c) Gassman P.G., van Bergen T.J., Oxindoles New, General Method of Synthesis, *J. Am. Chem. Soc.* **96(17)**: 5508–5512 (1974).

[6] (a) Wang Z., Zhang J., DFT Study on Structural, Electronic, and Vibrational Properties of the Highest Oxygenated Fullerene $C_{24}O_{12}$, *Comput. Theor. Chem.*, **972**:20–24 (2011).
(b) Tachikawa H., Iyama T., Abe S., DFT Study on the Interaction of Fullerene (C_{60}) with Hydroxyl Radical (OH), *Phys. Proc.*, **14**:139–142 (2011).
(c) Barszcz B., Laskowska B., Graja A., Park E.Y., Kim T.-D., Lee K.-S., Electronic Excitations of the Fullerene–Thiophene-Derived Dyads, *Syn. Met.* **161**:229–234 (2011).

[7] Woodard L.C., Li Z., Terrell J., Gerena L., Sanchez L.M., Kyle E.D., Bhattacharjee K.A., Nichols A.D., Ellis W., Prigge T.S., Geyer A.J., Waters N.C., Oxindole-Based Compounds are Selective Inhibitors of Plasmodium Falciparum Cycle Independent Protein Kinases, *J. Am. Chem. Soc.*, **46(18)**: 3877–3882 (2003).

[8] Cochard F., Laronze M., Prost É., Nuzillard J.-M., Augé F., Petermann C., Sigaut P., Sapi J., Laronze J.-Y., Synthesis of Substituted 1,2,3,4–Tetrahydro-1–thiacarbazole and Spiro[pyrrolidinone-3,3'-indolinones] through a Common Intermediate Obtained by Condensation of Indolin-2–one, (Aryl)aldehydes, and Meldrum's Acid, *Eur. J. Org. Chem.*, **2002**: 3481–3490 (2002).

[9] (a) Taylor R., Walton D.R.M., The Chemistry of Fullerenes, *Nature* **363**: 685–693 (1993).
(b) Prinzbach H., Weller A., Landenberger P., Wahl F., Worth J., Scott L.T., Gelmont M., Olevano D., Issendorff B., Gas-Phase Production and Photoelectron Spectroscopy of the Smallest Fullerene, C_{20}, *Nature*, **407**: 60–63 (2000).

[10] Kräutler B., Maynollo J., Diels-Alder reactions of the [60]fullerene Functionalizing a Carbon Sphere with Flexibly and with Rigidly Bound Addends, *Tetrahedron* **52**: 5033–5042 (1996).

[11] (a) Haerizade B.N., Ghavami M., Koohi M., Janitabar Darzi S., Rezaee N., Kasaei M.Z., Green Removal of Toxic Pb(II) from Water by a Novel and Recyclable Ag/γ-Fe_2O_3@r-GO Nanocomposite, *Iran. J. Chem. Chem. Eng. (IJCCE)* **37**:29–37 (2018).
(b) Koohi M., Shariati M., Soleimani Amiri S., A Comparative Study on the Ge_6C_{14} Heterofullerene Nanocages: A Density Functional Survey, *J. Phys. Org. Chem.* **30**: e3678–3687 (2017).

(c) Koohi M., Soleimani-Amiri S., Shariati M., Novel X- and Y-substituted Heterofullerenes $X_4Y_4C_{12}$ Developed from the Nanocage C_{20}, where X = B, Al, Ga, Si and Y = N, P, As, Ge: A Comparative Investigation on their Structural, Stability, and Electronic Properties at DFT, *Struct. Chem.* **29(3)**: 909–920 (2018).

(d) Ghavami M., Mohammadi R., Koohi M., Kassaee M.Z., Visible Light Photocatalytic Activity of Reduced Graphene Oxidesynergistically Enhanced by Successive Inclusion of γ-Fe_2O_3, TiO_2, and Ag Nanoparticles, *Mater. Sci. Semicond. Process.*, **26**: 69-78 (2014).

(e) Ghavami M., Koohi M., Kassaee M.Z., A Selective Nanocatalyst for an Efficient Ugi Reaction: Magnetically Rcoverable Cu(acac)$_2$/NH_2-T/SiO_2@Fe_3O_4 NPs, *J. Chem. Sci.* **125**:1347–1357 (2013).

(f) Ghavami M., Koohi M., Ahmadi A., Zandi H., Kassaee M.Z., Diastereoselective Synthesis of *N*-(*p*-Tosylsulfonyl)-2-Phenylaziridine Over a Novel Magnetically Recyclable Cu(II) Catalyst Accompanied with the *N*-Inversion Assessment at DFT, *Comb. Chem. High. T. Scr.* **17**:756–762 (2014).

(g) Koohi M., Kassaee M.Z., Ghavami M., Haerizade B.N., Ahmadi A.A., $C_{20-n}Ge_n$ Heterofullerenes (n = 5 - 10) on focus: A Density Functional Perspective, *Monatsh. Chem.*, **146**: 1409–1417 (2015).

(h) Koohi M., Soleimani Amiri S., Shariati M., Silicon Impacts on Structure, Stability and Aromaticity of $C_{20-n}Si_n$ heterofullerenes (n = 1 - 10): A Density Functional Perspective, *J. Mol. Struct.* **1127**:522–531 (2017).

(i) Baei M.T., Koohi M., Shariati M., Structure, Stability, and Electronic Properties of AlP Nanocages Evolved from the World's Smallest Caged Fullerene C_{20}: A Computational Study at DFT, *J. Mol. Struct.* **1159**:118–134 (2018).

[12] (a) Langa F., de la Cruz P., Espíldora E., García J.J., Pérez M.C., de la Hoz A., Fullerene Chemistry Under Microwave Irradiation, *Carbon*, **38(11-12)**: 1641–1646 (2000).

(b) Wu R., Lu X., Zhang Y., Zhang J., Xiong W., Zhu S., Addition Reactions of Fluoroalkanesulfonyl Azides to [60] Fullerene under Thermal or Microwave Irradiation Condition, *Tetrahedron* **64**: 10694–10698 (2008).

(c) Campisciano V., Riela S., Noto R., Gruttadauria M., Giacalone F., Efficient Microwave-Mediated Synthesis of Fullerene Acceptors for Organic Photovoltaics, *RSC Adv.* **4(108)**: 63200–63207 (2014).

(d) Shariatinia Z., Shahidi S., A DFT Study on the Physical Adsorption of Cyclophosphamide Derivatives on the Surface of Fullerene C_{60} Nanocage, *J. Mol. Graph. Model.*, **52**:71–81 (2014).

[13] (a) Koohi M., Bastami H., Structure, Stability, MEP, NICS, Reactivity, and NBO of Si—Ge Nanocages Evolved from C_{20} Fullerene at DFT, *Monatsh. Chem. – Chem. Month.* **151**: 693–710 (2020).

(b) Koohi M., Ghavami M., Haerizade B.N., Zandi H., Kassaee M.Z., Cyclacenes and Short Zigzag Nanotubes with Alternating Ge—C Bonds: Theoretical Impacts of Ge on the Ground State, Strain, And Band Gap, *J. Phys. Org. Chem.*, **27**: 735–746 (2014).

(c) Baei M.T., Koohi M., Shariati M., Characterization of C_{20} Fullerene and its Isolated $C_{20-n}Ge_n$ Derivatives (n = 1-5) by Alternating Germanium Atom(s) in Equatorial Position: A DFT Survey, *Heteroatom Chem.*, **29**: e21410–21423 (2018).

(d) Soleimani Amiri S., Koohi M., Mirza B., Characterizations of B, and N Heteroatoms as Substitutional Doping on Structure, Stability, and Aromaticity of Novel Heterofullerenesevolvedfrom the Smallest Fullerene Cage C_{20}: A Density Functional Theory Perspective, *J. Phys. Org. Chem.* **29**:514–522 (2016).

(e) Koohi M., Soleimani Amiri S., Haerizade B.N., Substituent Effect on Structure, Stability and Aromaticity of Novel $B_nN_mC_{20-(n+m)}$ Heterofullerenes, *J. Phys. Org. Chem.* **30**: e3682–3692 (2017).

(f) Soleimani-Amiri S., Koohi M., Azizi Z., Characterization of Nonsegregated $C_{17}Si_3$ Heterofullerenic Isomers Using Density Functional Theory Method, *J. Chin. Chem. Soc.*, **65**: 1453–1464 (2018).

(g) Ghavami M., Kassaee M.Z., Mohammadi R., Koohi M., Haerizadeh B.N., Fe_2O_3@Graphene Oxide as a Novel and Effective Visible Light Photocatalyst for Removal of Rhodamine b from Water, *Solid State Sci.*, **38**:143–149 (2014).

(h) Kassaee M.Z., Buazar F., Koohi M., Heteroatom Impacts on Structure, Stability and Aromaticity of X_nC_{20-n} Fullerenes: A Theoretical Prediction, *J. Mol. Struct. (THEOCHEM)*, **940**: 19–28 (2010).

[14] (a) Vessally E., Siadati S.A., Hosseinian A., Edjlali L., Selective sensing of Ozone and the Chemically Active Gaseous Species of the Troposphere by Using the C_{20} Fullerene and Graphene Segment, *Talanta* **162**:505–510 (2017).

(b) Vessally E., Soleimani–Amiri S., Hosseinian A., Edjlali L, Bekhradnia A., The Hartree–Fock Exchange Effect on the CO Adsorption by the Boron Nitride Nanocage, *Physica E*, **87**:308–311 (2017).

(c) Vessally E., Esrafili M.D., Nurazar R., Nematollahi P., Bekhradnia A., A DFT Study on Electronic and Optical Properties of Aspirin–Functionalized $B_{12}N_{12}$ Fullerene–Like Nanocluster, *Struct. Chem.*, **28**:735–748 (2017).

(d) Vessally E., Ahmadi E., Alibabaei S., Esrafili M.D., Hosseinian A., Adsorption and Decomposition of Formaldehyde on the $B_{12}N_{12}$ Nanostructure: A Density Functional Theory Study, *Monatsh. Chem.*, **148**:1727–1731 (2017).

(e) Nejati K., Hosseinian A., Vessally E., Bekhradnia A., Edjlali L., A Theoretical Study on the Electronic Sensitivity of the Pristine and Al-doped $B_{24}N_{24}$ Nanoclusters to F_2CO and Cl_2CO Gases, *Struct. Chem.*, **28**:1919–1926 (2017).

(f) Kareem R.T., Ahmadi S., Rahmani Z., Ebadi A.G., Ebrahimiasl S., Characterization of Titanium Influences on Structure and Thermodynamic Stability of Novel $C_{20-n}Ti_n$ Nanofullerenes (n = 1 - 5): A Density Functional Perspective, *J. Mol. Model.* **27(6)**: 176–187 (2021).

[15] (a) Hassanpour A., Youseftabar-Miri L., Delir Kheirollahi Nezhad P., Ahmadi S., Ebrahimiasl S., Kinetic Stability, and NBO Analysis of the $C_{20-n}Al_n$ Nanocages (n = 1 - 5) using DFT Investigation, *J. Mol. Struct.* **1233**:130079–130095 (2021).

(b) Hassanpour A., Yasar S., Ebadi A.G., Ebrahimiasl S., Ahmadi S., Thermodynamic Stability, Structural and Electronic Properties for the $C_{20-n}Al_n$ Heterofullerenes (n = 1 - 5): A DFT study, *J. Mol. Model.*, **27(5)**: 124–135 (2021).

(c) Hassanpour A., Delir Kheirollahi Nezhad P., Hosseinian A., Ebadi A.G., Ahmadi S., Ebrahimiasl S., Characterization of IR Spectroscopy, APT Charge, ESP Maps and AIM Analysis of C_{20} and its $C_{20-n}Al_n$ Heterofullerene Analogous (n = 1 - 5) Using DFT, *J. Phys. Org. Chem.* **34(7)**: e4198–4212 (2021).

(d) Vessally E., Soleimani–Amiri S., Hosseinian A., Edjlali L., Bekhradnia A., A Comparative Computational Study on the BN Ring Doped Nanographenes, *Appl. Surf. Sci.*, **396**: 740–745 (2017).

[16] (a) Becke A.D., Density-Functional Exchange-Energy Approximation with Correct Asymptotic Behavior, *Phys. Rev. A*, **38**: 3098–3100 (1988).

(b) Becke A.D., Density-Functional Thermochemistry. III. The Role of Exact Exchange, *J. Chem. Phys.* **98**:5648–5652 (1993).

(c) Becke A.D., Density-Functional Thermochemistry. IV. A New Dynamical Correlation Functional and Implications for Exact-Exchange Mixing, *J. Chem. Phys.*, **104**:1040–1046 (1996).

(d) Lee C., Yang W., Parr R.G., Development of the Colle-Salvetti Correlation-Energy Formula into a Functional of the Electron Density, *Phys. Rev. B*, **37**: 785–789 (1988).

[17] (a) Hariharan P.C., Pople J.A., Accuracy of AH_n Equilibrium Geometries by Single Determinant Molecular Orbital Theory, *J. Mod. Phys.* **27**:209–214 (1974).

(b) Francl M.M., Pietro W.J., Hehre W.J., Binkley J.S., Gordon M.S., DeFrees D.J., Pople J.A., Self-Consistent Molecular Orbital Methods. XXIII. A Polarization-Type Basis Set for Second Row Elements, *J. Chem. Phys.* **77**:3654–3665 (1982).

(c) Frisch M.J., Pople J.A., Binkley J.S., Self-Consistent Molecular Orbital Methods 25: Supplementary Functions for Gaussian Basis Sets, *J. Chem. Phys.*, **80**: 3265–3269 (1984).

(d) Clark T., Chandrasekhar J., Spitznagel G.W., Schleyer P.v.R., Efficient Diffuse Function-Augmented Basis Sets for Anion Calculations. III. the 3-21+G Set for first-row Elements, Li-F, *J. Comput. Chem.*, **4**: 294–301 (1983).

[18] (a) Schmidt M.W., Baldridge K.K., Boatz J.A., Elbert S.T., Gordon M.S., Jensen J.H., Koseki S., Matsunaga N., Nguyen K.A., Su S.J., Windus T.L., Dupuis M., Montgomery J.A., General Atomic and Molecular Electronic Structure System, *J. Comput. Chem.*, **14(11)**: 1347–1363 (1993).

(b) Sobolewski A.L., Domcke W., *Ab Initio* Investigation of the Structure and Spectroscopy of Hydronium−Water Clusters, *J. Phys. Chem. A*, **106**: 4158–4167 (2002).

[19] (a) Krishan R., Frisch M.J., Pople J.A., Contribution of Triple Substitutions to the Electron Correlation Energy in Fourth Order Perturbation Theory, *J. Chem. Phys.* **72**:4244–4245 (1980).
(b) Kendall R.A., Jr Dunning T.H., Harrison R.J., Electron Affinities of the First-Row Atoms Revisited. Systematic Basis Sets and Wave Functions, *J. Chem. Phys.*, **96**: 6796–6806 (1992).

[20] (a) Peng C., Schlegel H.B., Combining Synchronous Transit and Quasi-Newton Methods to Find Transition States, *Israel. J. Chem.* **33**:449–454 (1993).
(b) Peng C., Ayala P.Y., Schlegel H.B., Frisch M.J., Using Redundant Internal Coordinates to Optimize Equilibrium Geometries and Transition States, *J. Comput. Chem.*, **17**: 49–56 (1996).

[21] Hehre W.J., *Ab Initio* Molecular Orbital Theory, *Acc. Chem. Res.*, **9(11)**: 399–406 (1976).

[22] (a) Liu Q., Qiu L., Wang Y., Lv G., Liu G., Wang S., Lin J., Solvent Effect on Molecular Structure, IR Spectra, Thermodynamic Properties and Chemical Stability of Zoledronic Acid: DFT Study, *J. Mol. Model.*, **22**:84–94 (2016).
(b) Tsuru S., Sharma B., Nagasaka M., Hättig C., Solvent Effects in the Ultraviolet and X‑Ray Absorption Spectra of Pyridazine in Aqueous Solution, *J. Phys. Chem. A*, **125**:7198–7206 (2021).
(c) Sayyed-Alangi S.Z., Koohi M., Sajjadi-Ghotabadi H., Computational Study of Solvent Effects on Characterizations of (*E*)-3-X-Indoline-2-thiones Derivatives as Antivirus and Anticancer Compounds, *Bull. Korean Chem. Soc.* **36**:1985–1991 (2015).
(d) Soleimani-Amiri S., Koohi M., (*E*)-3-X-indoline-2-Ones as Potent and Selective Inhibitors Against Different Receptor Tyrosine Kinase (RTKs) in Solution *vs.* Gas Phase, at DFT, *J. Phys. Org. Chem.* **32(5)**: e3929–3943 (2019).

[23] (a) Biegler–König F., Schönbohm J., Update of the AIM2000-Program for Atoms in Molecules, *J. Comp. Chem.* **23**:1489–1494 (2002).
(b) Glendening E.D., Reed A.E., Carpenter J.E., Weinhold F., "NBO Version 3.1" Gaussian Inc., Pittsburgh. (2003).

[24] (a) Mohammadi M., Siadati S. A., Ahmadi S., Habibzadeh S., Poor Heravi M.R., Hossaini Z., Vessally E., Carbon Fixation of CO_2 via Cyclic Reactions with Borane in Gaseous Atmosphere Leading to Formic Acid (and Metaboric Acid); A Potential Energy Surface (PES) Study, *Front. Chem.*, **10** (2022).
(b) Gharibzadeh F., Vessally E., Edjlali L., Es' haghi M., Mohammadi R., A DFT Study on Sumanene, Corannulene and Nanosheet as the Anodes in Li−Ion Batteries, *Iran. J. Chem. Chem. Eng. (IJCCE)*, **39(6)**: 51-62 (2020).
(c) Afshar M., Khojasteh R.R., Ahmadi R., Nakhaei Moghaddam M., In Silico Adsorption of Lomustin Anticancer Drug on the Surface of Boron Nitride Nanotube, *Chem. Rev. Lett.*, **4**:178−184 (2021).
(d) Vessally E., Hosseinian A., A Computational Study on the Some Small Graphene-Like Nanostructures as the Anodes in Na−Ion Batteries, *Iran. J. Chem. Chem. Eng. (IJCCE)*, **40(3)**:6 91-703 (2021).
(e) Hashemzadeh B., Edjlali L., Delir Kheirollahi Nezhad P., Vessally E., A DFT Studies on a Potential Anode Compound for Li-Ion Batteries: Hexa-Cata-Hexabenzocoronene Nanographen, *Chem. Rev. Lett.*, **4**: 232-238 (2021).
(f) Vessally E., Farajzadeh P., Najaf, E., Possible Sensing Ability of Boron Nitride Nanosheet and Its Al– and Si–Doped Derivatives for Methimazole Drug by Computational Study, *Iran. J. Chem. Chem. Eng. (IJCCE)*, **40(4)**: 1001-1011 (2021).
(g) Majedi S., Sreerama L., Vessally E., Behmagham F., Metal-Free Regioselective Thiocyanation of (Hetero) Aromatic C-H Bonds using Ammonium Thiocyanate: An Overview, *J. Chem. Lett.*, **1**: 25-31 (2020).

[25] (a) Salehi N., Vessally E., Edjlali L., Alkorta I., Eshaghi M., Nan@Tetracyanoethylene (n=1-4) Systems: Sodium Salt Vs Sodium Electride, *Chem. Rev. Lett.*, **3**: 207-217 (2020).
(b) Soleimani-Amiri S., Asadbeigi N., Badragheh S., A Theoretical Approach to New Triplet and Quintet (nitrenoethynyl) alkylmethylenes,(nitrenoethynyl) alkylsilylenes,(nitrenoethynyl) alkylgermylenes, *Iran. J. Chem. Chem. Eng. (IJCCE)*, **39(4)**: 39-52 (2020).

(c) Sreerama L., Vessally E., Behmagham F., Oxidative Lactamization of Amino Alcohols: An Overview, *J. Chem. Lett.*, **1**: 9-18 (2020).
(d) Norouzi N., Ebadi A. G., Bozorgian A., Vessally E., Hoseyni S. J., Energy and Exergy Analysis of Internal Combustion Engine Performance of Spark Ignition for Gasoline, Methane, and Hydrogen Fuels, *Iran. J. Chem. Chem. Eng. (IJCCE)*, **40(6)**: 1909-1930 (2021).
(e) Kamel M., Mohammadifard, M., Thermodynamic and Reactivity Descriptors Studies on the Interaction of Flutamide Anticancer Drug with Nucleobases: A Computational View, *Chem. Rev. Lett.*, **4**: 54-65 (2021).
(f) Vessally E., Musavi M., Poor Heravi M.R., A Density Functional Theory Study of Adsorption Ethionamide on The Surface of the Pristine, Si and Ga and Al-Doped Graphene, *Iran. J. Chem. Chem. Eng. (IJCCE)*, **40(6)**: 1720-1736 (2021).
(g) Vakili M., Bahramzadeh V., Vakili M., A Comparative study of SCN- adsorption on the $Al_{12}N_{12}$, $Al_{12}P_{12}$, and Si and Ge -doped $Al_{12}N_{12}$ nano-cages to remove from the environment, *J. Chem. Lett.* 1:172−178 (2020)

[26] (a) Mosav, M., Adsorption Behavior of Mephentermine on the Pristine and Si, Al, Ga- Doped Boron Nitride Nanosheets: DFT Studies, *J. Chem. Lett.*, **1**: 164-171 (2020).
(b) Vessally E., Siadati S.A., Hosseinian A., Edjlali L., Selective Sensing of Ozone and the Chemically Active Gaseous Species of the Troposphere by Using the C20 Fullerene and Graphene Segment, *Talanta*, **162**: 505-510 (2017).
(c) Norouzi N., Ebadi A. G., Bozorgian A., Hoseyni S.J., Vessally E., Cogeneration System of Power, Cooling, and Hydrogen from Geothermal Energy: An Exergy Approach, *Iran. J. Chem. Chem. Eng. (IJCCE)*, **41(2)**: 706-721 (2022).
(d) Rabipour S., Mahmood E.A., Afsharkhas M., A Review on the Cannabinoids Impacts on Psychiatric Disorders, *Chem. Rev. Lett.*, **5**: (2022).
(e) Siadati S.A., Vessally E., Hosseinian A., Edjlali L., Possibility of Sensing, Adsorbing, and Destructing the Tabun-2D-Skeletal (Tabun Nerve Agent) by C20 Fullerene and its Boron and Nitrogen Doped Derivatives, *Synthetic Metals*, **220**: 606-611 (2016).
(f) Rabipour S., Mahmood E.A., Afsharkhas M., Medicinal Use of Marijuana and Its Impacts on Respiratory System, *J. Chem. Lett.*, **3**: 86-94 (2022).